This article was published in International Journal of Hydrogen Energy, 40(20), 6566-6572, 2015
http://dx.doi.org/10.1016/j.ijhydene.2015.03.106

Surface effects and CO/CO2 influence in the H2 permeation through a Pd-Ag membrane: A comprehensive model

Patricia Perez [a], Carolina A. Cornaglia [b], Adelio Mendes [a], Luis M. Madeira [a], Silvano Tosti [c]

[a] *LEPABE - Chemical Engineering Department, Faculty of Engineering, University of Porto, Rua Dr. Roberto Frias, s/n, 4200-465 Porto, Portugal*

[b] *INCAPE - Research Institute on Catalysis and Petrochemistry, Chemical Engineering Department, University of the Litoral, Santiago del Estero 2829, 3000 Santa Fe, Argentina*

[c] *ENEA - Technical Unit for Nuclear Fusion, Frascati, Via E. Fermi 45, Frascati, Roma I 00044, Italy*

Abstract

The permeability of a 0.175 mm thick Pd-Ag tubular membrane to pure H2 and binary mixtures of H2/CO or H2/CO2 was studied. The tests were performed in a wide range of temperature (523-723 K) and pressure (200-800 kPa).

Pure H2-permeation through a dense metal membrane is described by the Sieverts' law. However, it was already found that the H2 permeation does not follow the Sieverts' law when other components are present in the feed and namely CO or CO2. In this work, it is proposed a new permeation model based on the Sieverts' law considering: i) the mass transfer resistance due to the surface effects and ii) the barrier effect due to the presence of either CO or CO2. The model was successfully validated against experimental data of hydrogen permeation for binary (H2/CO and H2/CO2) experiments for every working temperature and pressure.

Introduction

The exploitation of fossil fuels is not sustainable for a long time because of their impact on the environment. In fact, the combustion of these fuels generates greenhouse gases that contribute to global warming, caused by their accumulation in the atmosphere, for example CO2 [1]. In this context the need comes up for a global action to decrease the pollution levels and implement

environmentally friendly energy technologies (e.g. solar, wind, geothermal, etc.). There are some types of applications (e.g. propulsion of cars, buses, laptop batteries, cell phones, etc.) where it is necessary to use an intermediate energy carrier. It is in this sense that hydrogen is so attractive [2]. The use of hydrogen as a clean energy vector is every day more recurrent: combustion of hydrogen results in water and, particularly, its environmental impact is very limited when produced from renewables [3-5]. Currently, the principal source of hydrogen is the reforming of hydrocarbons, mainly methane [6]. As a result of the methane steam reforming some compounds like CO, CO_2, H_2O, etc. are obtained together with H_2. In several uses, high purity hydrogen streams are important, for example for fuel cells or nuclear applications. In these cases is mandatory purifying and separating the hydrogen from the syngas stream. For this purpose, several technologies can be applied such as, cryogenic cooling, PSA and H_2-selective membranes [7].

Methods of separation/purification by H_2-selective membranes are increasingly attractive as compared to other technologies because of their modularity, low energy consumption, possibility for continuous and easy operation, and finally cost effectiveness [8]. Pd-based membranes are particularly interesting due to their high hydrogen permeance and good selectivity [9]. Pure palladium membranes are prone to suffer from the embrittlement phenomenon that can be significantly reduced by alloying Pd with other metals (Ag, Au, Cu, etc.). Self-supported Pd∈Ag membranes consisting of dense tubes have been developed for separating ultra-pure hydrogen. Particularly, Pd-Ag thin wall permeator tubes produced via cold-rolling and diffusion welding of metal foils have been produced and characterized in long term permeation tests, demonstrating their complete hydrogen selectivity and durability [10∈12]. These dense Pd-Ag tubes have been used in membrane reactors where several dehydrogenation reactions take place; ultra-pure hydrogen production as well as high hydrogen yields have been obtained [13,14].

In most cases, the H_2-permeation through a Pd-membrane is described by the Sieverts' law (Eq. (1)):

$$J_{H_2} = \frac{P_e}{d}\left(p_{H_2,up}^{0.5} - p_{H_2,down}^{0.5}\right) \qquad (1)$$

where JH_2 is the H_2-flux through the membrane (mol $s^{-1}m^{-2}$), Pe is the permeability of the membrane (mol s^{-1} m^{-1} $Pa^{-0.5}$), d is the membrane

thickness (m), $pH2;up$ is the upstream H2- partial pressure (in the feed stream, Pa) and $pH2$;*down* is the downstream H2-partial pressure (in the permeate side, Pa). According to the Sieverts' law, the pressure dependence factor (n) of the hydrogen flux on the H2-partial pressure has the value of 0.5.

However, there are several references in the literature about deviations from this law. Deviations from the ideal behavior predicted by the Sieverts' law are due to different factors: poisoning of the membrane surface, membrane defects, mass transfer resistance phenomena related to the surface effect, etc. [15-18].

In this work, a comprehensive approach derived from the Sieverts' law is proposed. This new model takes into account two of the main reasons for deviation of Sieverts' law: i) the barrier effect of CO or CO2 on the surface of the membrane and ii) the mass transfer resistance due to hydrogen adsorption/desorption over the metal surface. Species such as CO and CO2 cause the deactivation of the membrane because they can block the hydrogen adsorption sites. On the other hand, the mechanism of hydrogen transport through a dense mem- brane comprises several stages and, practically, it is controlled by the adsorption/desorption rates over the metal surface and by the diffusion through the metal lattice. Therefore, the effects of surface reactions should be considered in the hydrogen permeation models since they can significantly affect the hydrogen mass transfer resistance. The novel approach proposed in this work was validated by experimental data in a wide range of operating conditions.

Experimental

In order to characterize a tubular Pd/25%Ag-membrane several permeation tests were carried out. The permeation tests were conducted at ENEA Frascati laboratories using a dense Pd-Ag tubular membrane having the following dimensions: 10 mm of internal diameter, 0.175 mm (175 μm) of wall thickness and 125 mm of length. The membrane tube was joined at its ends to two stainless steel tubes in order to form the *permeator* tube shown in Fig. 1.

In all cases, for H2-pure as for binary mixtures tests (H2/CO and H2/CO2), the hydrogen flux permeating through the membrane has been measured in the pressure and temperature ranges of 200-800 kPa and 523-723 K, respectively. All experiments were carried out at a constant total feed flow rate (FT) of 700 $mL_N\ min^{-1}$ and the hydrogen permeated through the membrane was collected by a constant sweep gas stream of nitrogen (50 $mL_N\ min^{-1}$) sent in counter-current mode in the shell side (Fig. 2).

The permeator tube was wrapped by a Pt-wire electric resistance, which was used to heat the membrane until the working temperature; a thermocouple was located very near from the permeator tube external surface to measure the temperature. All this was assembled inside a Pyrex tube (in the shell) in a finger-like configuration accordingly to a well- established and proven membrane module design [19]. One end of the permeator tube is sealed while the other one allows the placing of a stainless steel channel which is responsible for supplying the feed gas mixture. More details about the module and the experimental set-up are given in Fig. 2. In order to thermally isolate the membrane module and keep constant the working temperature, the Pyrex shell was covered with a quartz wool blanket. The feed stream consisting of high purity gases enters into the permeator lumen side through a mass flow controller (MFC). The permeate stream flow rate consisting of ultra-pure hydrogen was measured by a mass flow meter (MFM). Pressure was measured at the inlet/outlet of the permeator lumen and at the shell outside (PI) by pressure gages. The lumen pressure was controlled through a throttle valve (TV).

Selectivity to hydrogen of the membrane has been verified by gas-chromatographic measurements of the permeate and its tightness checked by pressuring the membrane lumen with inert gas during the night.

For the binary mixtures, tests were performed by feeding the membrane with streams of different compositions of H_2/ CO or H_2/CO_2, as shown in Table 1.

Results and discussion

Pure hydrogen permeation tests

Pure hydrogen tests were conducted to measure the hydrogen permeability under specific and controlled temperature and pressure conditions.

Fig. 3 shows that the Arrhenius' plot of the H_2-permeability is represented by different curves for each feed pressure when applying the Sieverts' law model of Eq. (1).

Actually, from the Sieverts' law the permeability should be independent of the total pressure, thus demonstrating that such a model is not effective to describe the permeation phenomena in the experienced pressure range (200-800 kPa). This effect is more noticeable for lower temperatures; similar results have been reported elsewhere [20].

In order to more accurately calculate the permeability of the membrane, a modified model that introduces in the Sieverts' law the surface mass transfer resistance and the logarithmic mean driving force was considered (Eqs. (2)-(4)).

The surface mass transfer resistance is due to the hydrogen adsorption/desorption reactions over the metal surfaces. Further, the hydrogen partial pressure in the permeate side is not constant along the axial coordinate because of the continuous removal of hydrogen and an appropriate expression of the driving force has to be used. By analogy of the mathematical equation used to describe the temperature gradient in a heat exchanger, it is possible to express the H2- permeating driving force as a similar expression but, in terms of pressure gradient, that is as a log mean of the H2-partial pressure difference [21].

$$J_{H_2} = \frac{P_e}{d} \Delta P_{ln} \qquad (2)$$

$$\Delta P_{ln} = \frac{\left[\left(p_{H_2,feed} - J_{H_2}R_s\right)^{0.5} - \left(p_{H_2,perm\ out} + J_{H_2}R_s\right)^{0.5}\right] - \left[\left(p_{H_2,ret} - J_{H_2}R_s\right)^{0.5} - \left(p_{H_2,perm\ in} + J_{H_2}R_s\right)^{0.5}\right]}{A} \qquad (3)$$

$$A = \ln\left\{\frac{\left(p_{H_2,feed} - J_{H_2}R_s\right)^{0.5} - \left(p_{H_2,perm\ out} + J_{H_2}R_s\right)^{0.5}}{\left(p_{H_2,ret} - J_{H_2}R_s\right)^{0.5} - \left(p_{H_2,perm\ in} + J_{H_2}R_s\right)^{0.5}}\right\} \qquad (4)$$

In Eqs. (2)-(4), $pH_{2,feed}$ is the H2-partial pressure at the inlet of membrane lumen (Pa), $pH_{2,ret}$ is the H2-partial pressure at the outlet of membrane lumen (Pa), $pH_{2,perm\ in}$ is the H2-partial pressure at the inlet of permeate side (Pa), $pH_{2,perm\ out}$ is the H2- partial pressure at the outlet of the permeate side (Pa), R_S is the surface mass transfer resistance (mol^{-1} m^2 s Pa). According to the Sieverts' law, the pressure dependence factor (n) of the hydrogen flux on the H2-partial pressure has the value of 0.5. Particularly, for pure-hydrogen tests, $pH_{2,feed} = pH_{2,ret}$; for our configuration (sweep gas stream in counter-current mode), $pH_{2,perm\ in}$ is null.

Then, the permeability of the membrane can be assessed from this new expression (Eqs. (2)-(4)) as long as R_S is known. In this work, the values of R_S were taken as an average for ranges according to the literature for membranes of identical composition and similar thicknesses (ca. 200 μm) [20,22] - see Table 2 where the calculated values of hydrogen permeability are also reported.

Contrarily to what happens with Pe values, R_S increases when the temperature decreases (Table 2); actually, the resistance to the H2-permeation increases exponentially with the temperature decrease.

Accordingly, the permeability vs. temperature can be written by the expression [23]:

$$P_e = P_{e_0} e^{-\frac{E_a}{RT}} \quad (5)$$

where Pe_0 is the pre-exponential coefficient (mol m^{-1} s^{-1} $Pa^{-0.5}$), Ea is the activation energy of permeation (J mol^{-1}), R is the universal gas constant (J mol^{-1} K^{-1}) and T is the absolute temperature (K). Through the fitting, it was determined the values of Pe_0 and Ea to be 2.61×10^{-8} mol m^{-1} s^{-1} $Pa^{-0.5}$ and 2.09×10^{3} J mol^{-1} respectively.

Values of the hydrogen permeability obtained in this work are comparable with those reported in the literature for similar membranes as shown in Table 3.

Effect of CO or CO2 in the H2 permeation tests

Some species like CO and CO_2 interact with the metals and are adsorbed on their surface. As a consequence some sites available for the hydrogen dissociation over the metal surface may be blocked, thus causing a reduction of the membrane active area.

In a previous work, the presence of poisoning gases on the hydrogen permeation through Pd-membranes has been taken into account by a model described therein [21]. Such a model has been now further modified by introducing the logarithmic mean driving force defined by Eqs. (3) and (4), thus obtaining a comprehensive expression accounting for both the surface and poisoning effects:

$$J_{H_2} = \frac{P_e}{d}\left(1 - \alpha \frac{K_i \overline{p_i}}{1 + K_i \overline{p_i}}\right) \Delta P_{ln} \quad (6)$$

where the parameter α (dimensionless) depends only on the temperature and accounts for additional effects of the adsorbed gas, Ki is the adsorption equilibrium constant (Pa^{-1}) and pi is the average partial pressure (Pa) of species i.

In order to account the inhibitor effect of the CO or CO_2 on the hydrogen permeability, the α and Ki parameters were linear fitting of the experimental data reported in Figs. 4 and 5; the values obtained are shown in Table 4.

As expected, both a and K decrease with temperature (the last one

corresponding to a van't Hoff behavior) being the adsorption equilibrium constants much larger for CO than for CO_2, as reported elsewhere [21].

The poisoning effect of CO/CO on the H -permeation flux can be highlighted by assessing the normalized fluxes of H_2 (Eq. (7)) versus the percentage of each of these substances in the feed stream. The normalized flux of hydrogen J^*_{H2} is calculated by the following expression:

$$J^*_{H_2} = \frac{J_{H_2/CO \text{ or } CO_2}}{J_{H_2}} \qquad (7)$$

where: $J_{H2/CO\ or\ CO2}$ (mol $s^{-1} m^{-2}$) is the hydrogen permeation flux measured in the H_2/CO or H_2/CO_2 tests and J_{H2} is the hydrogen permeation flux calculated via Eq. (2) with the values of the hydrogen partial pressures measured in the CO/ CO_2 tests (i.e., taking into account the decrease of the hydrogen partial pressure when increasing the feed concentration of such gases); this way the driving force is the same in both terms.

The experimental data shown by Figs. 4 and 5 were obtained at a feed total pressure of 500 kPa. The fitting obtained by the novel approach (Eq. (6)) and with the parameters given in Tables 2 and 4 is shown as dashed lines. A very good adherence is observed. The same happens for other pressures (data not shown).

In both graphs the H_2-permeation fluxes are lower than the ones reached with pure H_2. The inhibitory effect is in general more pronounced for CO than for CO_2; this result suggests that the interaction of CO with the Pd-Ag surface is stronger than that of CO_2 in the range of temperature studied. Also, the inhibitory effect increases with the amount of CO (or CO_2) in the mixed feed because, in the tested conditions, the CO (or CO_2) coverage of the metal surface is directly related to the CO (or CO_2) concentration in the gas phase. Finally, at high CO concentration it is perceptible that an asymptotic trend is observed, not seen for the curves of CO_2 mixtures. A similar trend has been reported before in the literature [21], and is related with the much higher adsorption equilibrium constants for CO (cf. Table 4).

Figs. 4 and 5 show that, in agreement with the literature [21,26], the inhibition effect of CO/CO_2 decreases with temperature. Moreover, it is observed that for CO there is a high gap between the normalized hydrogen fluxes at 673 and 573 K as compared with other temperatures. This is related with the mechanism of the gases interaction with the metallic surface (as inferred from the adsorption enthalpies), as detailed below.

The adsorption enthalpy for each gas (ΔH_i) was determined by using the van't

Hoff equation.

$$\frac{d\ln(K_i)}{d\left(\frac{1}{T}\right)} = -\frac{\Delta H_i}{R} \quad (8)$$

According with Fig. 6, the adsorption enthalpy obtained for CO_2 is -17.85 kJ mol^{-1}. This value is higher than that reported previously for a 50 μm thick Pd-Ag membrane (-5.41 kJ mol^{-1}) [21], thus indicating that some contribution of chemical sorption might occur in the herein obtained data [27,28], recorded at higher temperatures. For CO, it seems that there is a change in the mechanism with temperature, with an adsorption enthalpy of -2.10 kJ mol^{-1} at higher temperatures (Section 1), and -45.63 kJ mol^{-1} at lower ones (Section 2). This explains the gap observed in Fig. 4.

In a previous work the reversibility of the CO/CO_2 effects was analyzed [21]. In the case of CO_2 it was possible to recover completely the initial flux by passing N_2 on both sides of the membrane, while after using CO a treatment with synthetic air at 573 K was required to restore the membrane permeance towards H_2. In this work the same procedure was required. It appears that the reaction of oxygen with the adsorbed CO produces CO_2 that is purged, leading to complete membrane regeneration.

Conclusions

The hydrogen permeation flux through dense metal mem- branes is normally studied using the Sieverts' law but, this model is not always accurate enough. This is the case when other effects prevail, like presence of inhibitor gases (e.g. CO and CO_2) and/or surface mass transfer resistances. Because of this, it has been proposed a new model able to predict the H_2- permeation tendency with a high level of accuracy for the studied conditions (presence of inhibitor gases, wide ranges of pressure and temperature).

The model has shown an adequate fit to the experimental data (CO/H_2 and CO_2/H_2 mixtures) by successful validation in the large range of experienced conditions. Permeability towards pure hydrogen of a Pd-Ag self-supported membrane has been determined, taking the surface transfer resistance coefficients as the average from literature values. Particularly, in experiments with pure hydrogen the Pe_0 and Ea values were calculated, which were consistent with those reported in the literature. It was equally proved the

inhibitory effect of CO and CO_2 on the H_2-permeating flux. Such an effect decreases with temperature and increases with the CO/CO_2 composition in the feed.

The adsorption enthalpy values obtained, ΔHCO; ΔHCO_2, are low, suggesting that weak physical sorption phenomena occur.

Acknowledgments

Luis M. Madeira and Adélio Mendes acknowledge that this work has been made possible by FEDER's funds through the Operational Program for Competitiveness Factors - COMPETE - and national funds through FCT - Foundation for Science and Technology - under the project with reference PTDC/EQU-ERQ/098730/2008. Patricia Pérez also thanks to the same institutions for funding received through the Doctoral Grant (SFRH/BD/73673/2010). Carolina Cornaglia wishes to acknowledge the UNL, CONICET, ANPCYT, UNIROMA and the Erasmus program for the financial support.

References

1. Schurer AP, Hegerl GC, Mann ME, Tett SFB, Phipps SJ. Separating forced from chaotic climate variability over the past millennium. J Clim 2013;26:6954-73.
2. Cârdu M, Baica M. Hydrogen - the ecologically ideal energy vector. In: Environmental science: alternative fuel. InTech; 2011. p. 335e46 [Chapter 14].
3. Mansilla C, Avril S, Imbach J, Le Duigou A. CO_2-free hydrogen as a substitute to fossil fuels: what are the targets? prospective assessment of the hydrogen market attractiveness. Int J Hydrogen Energy June 2012;37(12):9451-8.
4. Orhan Mehmet F, Dincer Ibrahim, Rosen Marc A, Kanoglu Mehmet. Integrated hydrogen production options based on renewable and nuclear energy sources. Renew Sustain Energy Rev October 2012;16(8):6059-82.
5. Nowotny J, Veziroglu TN. Impact of hydrogen on the environment. Int J Hydrogen Energy 2011;36:13218-24.
6. Assaf EM, Jesus CDF, Assaf JM. Mathematical modelling of methane steam reforming in membrane reactor: an isothermic model. Braz J Chem Eng 1998;15. http://dx.doi.org/ 10.1590/S0104-66321998000200010.
7. Uehara I. Separation and purification of hydrogen. In: Energy carriers and conversion systems with emphasis on hydrogenvol. 1; 2008. p. 268-82. Tokio: Tokio Ohta.

8. Ockwig NW, Nenoff TM. Membranes for hydrogen separation. Chem Rev 2007;107:4078-110.
9. Zhang Yi, Lu Jian, Maeda Ryutaro, Nishimura Chikashi. Hydrogen permeation of thin Pd-25Ag membranes prepared by cold rolling and microsystem technology. Mater Trans 2008;49(4):754-9.
10. Tosti S. Method of diffusion bonding thin foils made of metals alloys selectively permeable to hydrogen, particularly providing membrane devices, and apparatus for carrying out the same. European Patent EP 1184125 B1. 2001.
11. Tosti S, Bettinali L. Diffusion bonding of Pd-Ag rolled membranes. J Mater Sci 2004;39:3041-6.
12. Tosti S, Basile A, Bettinali L, Borgognoni F, Chiaravalloti F, Gallucci F. Long-term tests of Pd-Ag thin wall permeator tube. J Membr Sci 2006;284:393-7.
13. Tosti S. Overview of Pd-based membranes for producing pure hydrogen and state of art at ENEA laboratories. Int J Hydrogen Energy 2010;35:12650-9.
14. Mendes D, Chibante V, Zheng J-M, Tosti S, Borgognoni F, Mendes A, et al. Enhancing the production of hydrogen via water-gas shift reaction using Pd-based membrane reactors. Int J Hydrogen Energy 2010;35:12596-608.
15. Hara S, Ishitsuka M, Suda H, Mukaida M, Haraya K. Pressure- dependent hydrogen permeability Extended for metal membranes not obeying the square-Root law. J Phys Chem B 2009;113:9795-801.
16. Ward TL, Dao T. Model of hydrogen permeation behavior in palladium membranes. J Membr Sci 1999;153:211-31.
17. Morreale BD, Ciocco MV, Enick RM, Morsi BI, Howard BH, Cugini AV, et al. The permeability of hydrogen in bulk palladium at elevated temperatures and pressures. J Membr Sci 2003;212:87-97.
18. Guazzone F, Engwall EE, Ma YH. Effects of surface activity, defects and mass transfer on hydrogen permeance and n- value in composite palladium-porous stainless steel membranes. Catal Today 2006;118:24-31.
19. Tosti S, Basile A, Bettinali L, Borgognoni F, Gallucci F, Rizzello C. Design and process study of Pd membrane reactors. Int J Hydrogen Energy 2008;33:5098e105.
20. Vadrucci M, Borgognoni F, Moriani A, Santucci A, Tosti S. Hydrogen permeation through PdeAg membranes: surface effects and Sievert's Law. Int J Hydrogen Energy 2013;38:4144-52.
21. Miguel CV, Mendes A, Tosti S, Madeira LM. Effect of CO and CO_2 on H_2 permeation through finger-like PdeAg membranes. Int J Hydrogen Energy 2012;37:12680-7.
22. Serra E, Kemali M, Perujo A, Ross DK. Hydrogen and deuterium in Pd-25 Pct Ag alloy: permeation, diffusion, solubilization and surface reaction. Metall

Mater Trans A 1998;29 A:10223-1027.
23. Robeson LM. Polymer membranes for gas separation. Curr Opin Solid State Mater Sci 1999;4:549-52.
24. Ackerman FJ, Koskinas GJ. Permeation of hydrogen and deuterium through palladium-silver alloys. J Chem Eng Data 1972;17:51-5.
25. Yoshida H, Konishi S, Naruse Y. Preliminary design of a fusion reactor fuel cleanup system by the palladium-alloy membrane method. Nucl Technol/Fusion 1983;3:471-84.
26. Amano M, Nishimura C, Komaki M. Effects of high concentration CO and CO2 on hydrogen permeation through the palladium membrane. Mater Trans 1990;31:404-8.
27. Atkins P, de Paula J. Atkins' physical chemistry. 8th ed. New York: W. H. Freeman and Company; 2006.
28. Keller JU, Staudt R. Adsorption isotherms. In: Keller JU, Staudt R, editors. Gas adsorption equilibria: experimental methods and adsorptive isotherms. Boston: Springer Science þ Business Media, Inc; 2005. p. 359-413.

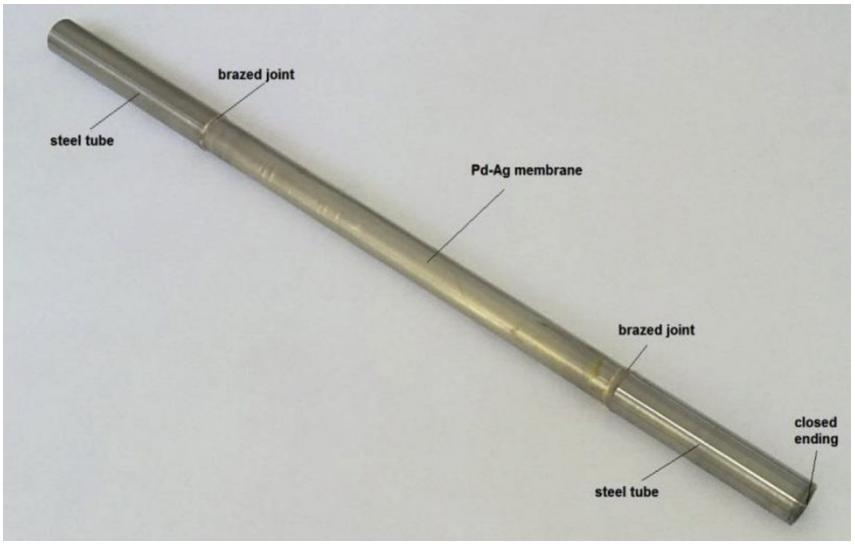

Fig. 1 - Pd-Ag permeator tube.

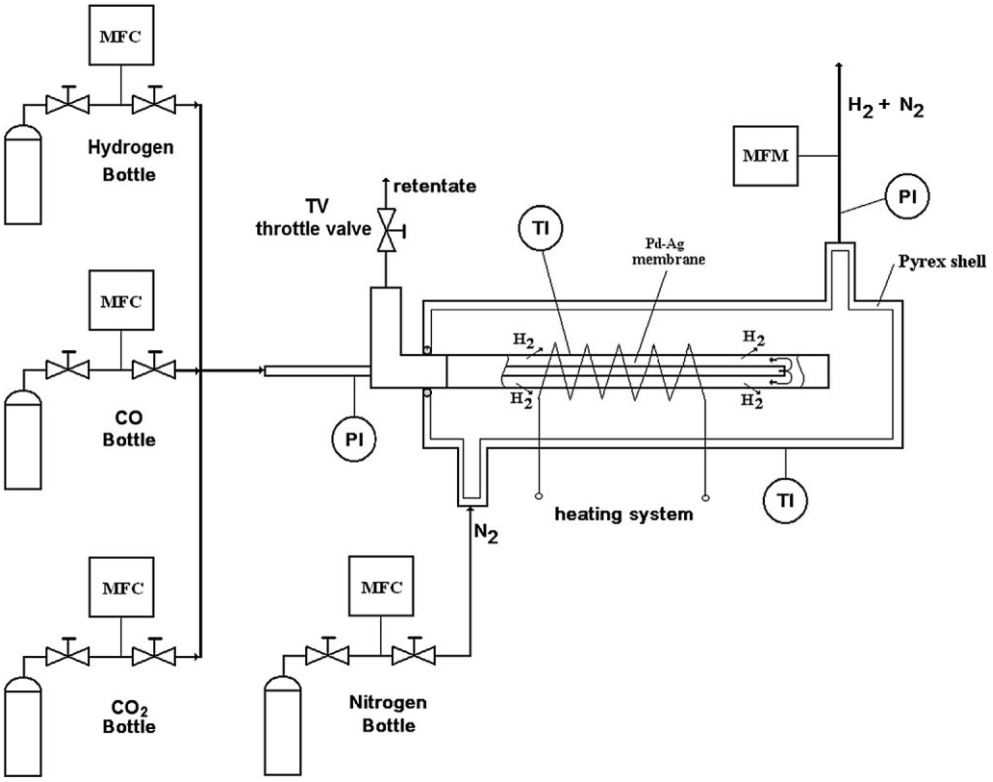

Fig. 2 - Scheme of the membrane module and of the experimental set-up.

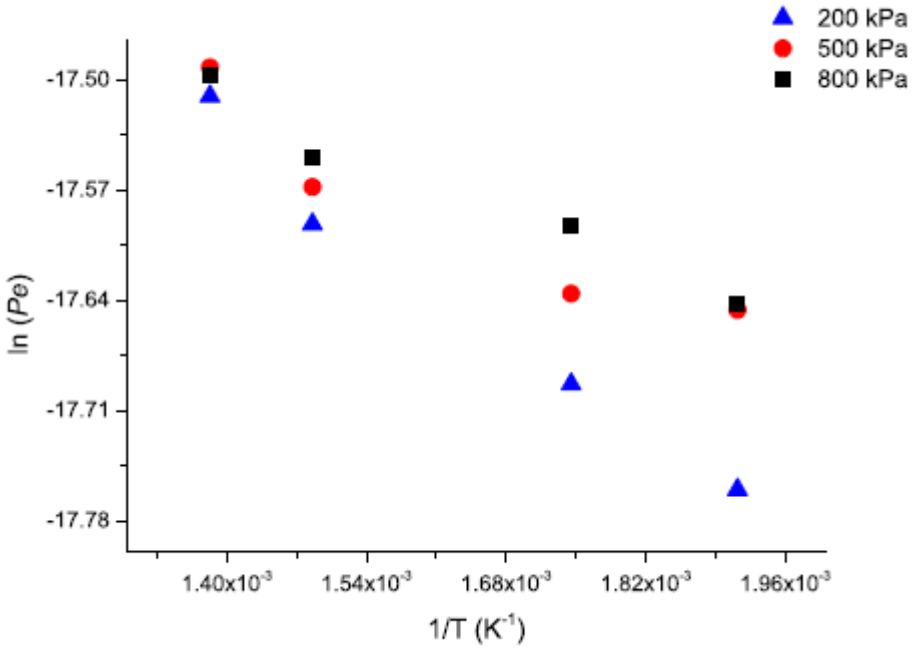

Fig. 3 - Arrhenius plot of the permeability obtained using the Sieverts' law (Eq. (1)) at different hydrogen feed pressures

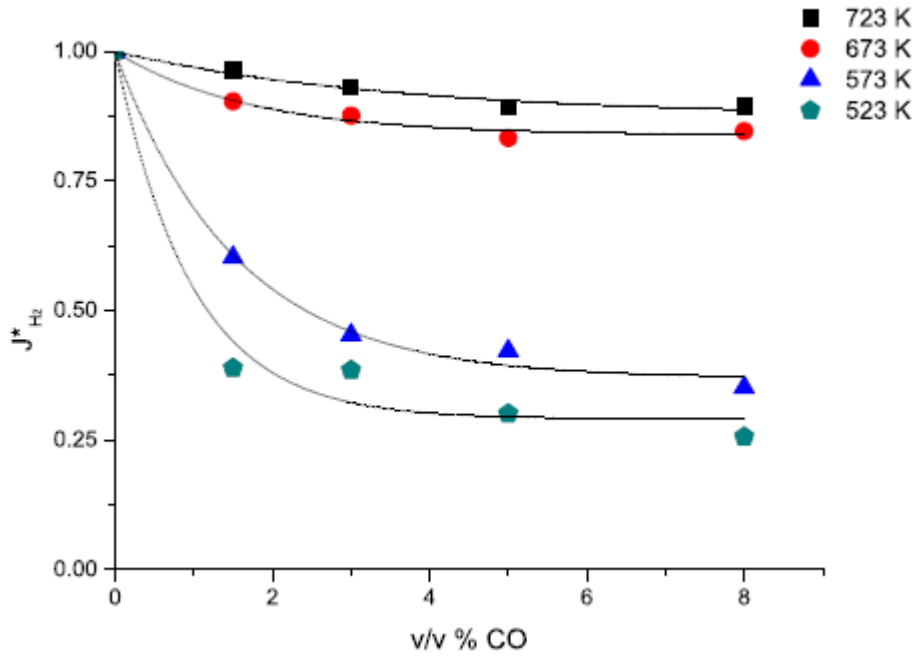

Fig. 4 - Normalized H2-flux vs %CO in the feed stream. The fitted function (dashed lines) is based on the new model (Eq. (6)).

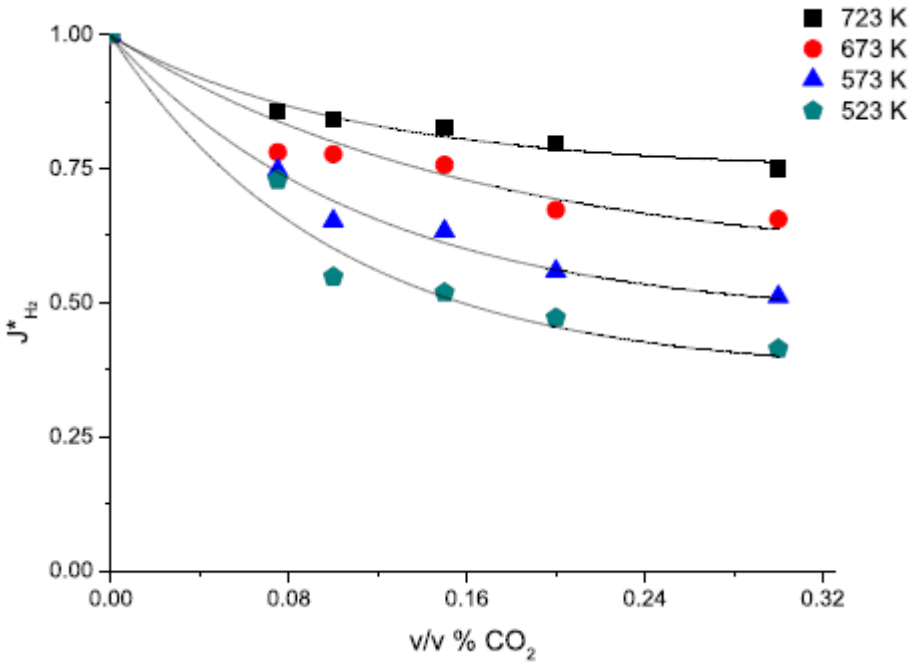

Fig. 5 - Normalized H2-flux vs %CO2 in the feed stream. The fitted function (dashed lines) is based on the new model (Eq. (6)).

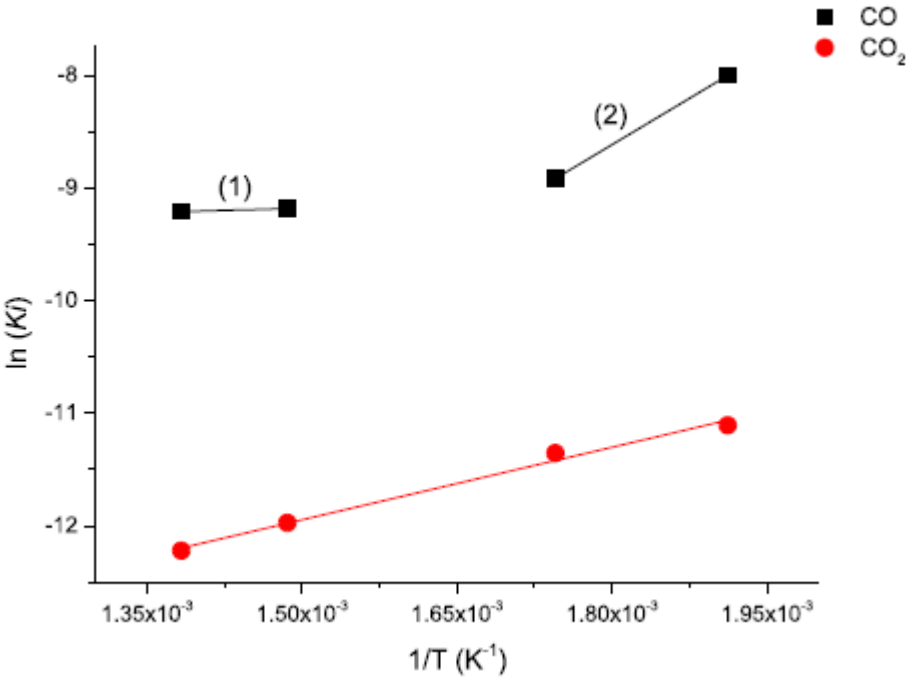

Fig. 6 - Linear regression between the determined adsorption constants of CO and CO2 versus the inverse of temperature

Table 1 – - Composition of the feed stream during the binary experiments[a].

Composition	CO (%)	CO_2 (%)	H_2 (%)
CO/H_2	1.5–8.0	–	98.5–92.0
CO_2/H_2	–	7.5–30.0	92.5–70.0

[a] $F_T = 700\ mL_N\ min^{-1}$, sweep gas ($50\ mL_N\ min^{-1}$).

Table 2 – Values of mass transfer resistance (R_s) obtained from literature [20,22] and permeability (P_e) calculated in this work by Eqs. (2)–(4).

T (K)	R_s ($mol^{-1}\ m^2\ s\ Pa$)	P_e ($mol\ m^{-1}\ s^{-1}\ Pa^{-0.5}$)
723	1.10×10^4	1.88×10^{-8}
673	1.46×10^4	1.77×10^{-8}
573	3.00×10^4	1.66×10^{-8}
523	78.78×10^4	1.64×10^{-8}

Table 3 – - Calculated hydrogen permeability and comparison with literature.

P_{e0} (mol m^{-1} s^{-1} Pa$^{-0.5}$)	E_a (J mol^{-1})	P_{feed} (kPa)	T (K)	d (μm)	Ref.
2.06×10^{-8}	2.59×10^{3}	200–800	473–623	200	[20]
5.58×10^{-8}	6.30×10^{3}	1–100	50–500	198	[22]
7.73×10^{-8}	6.60×10^{3}	680–6800	300–500	125	[24]
3.85×10^{-8}	5.75×10^{3}	120–870	380–580	80	[25]
2.61×10^{-8}	2.09×10^{3}	200–800	523–723	175	(This work)

Table 4 – The α and Ki parameters of Eq. (6) obtained by fitting the experimental data of Figs. 4 and 5.

T (K)	CO		CO_2	
	α	K (Pa^{-1})	α	K (Pa^{-1})
723	0.12	1.00×10^{-4}	0.62	4.93×10^{-6}
673	0.20	1.03×10^{-4}	0.77	6.30×10^{-6}
573	0.77	1.34×10^{-4}	0.80	1.17×10^{-5}
523	0.78	3.35×10^{-4}	0.90	1.50×10^{-5}